Pigment Mapping of the Scream (1893) Based on Hyperspectral Imaging

Hilda Deborah*, Sony George, and Jon Yngve Hardeberg

The Norwegian Colour and Visual Computing Laboratory
Gjøvik University College, P.O. Box-191
2802, Gjøvik, Norway

Abstract. Hyperspectral imaging is a promising non-invasive method for applications in conservation of painting. With its ability to capture both spatial and spectral information which relates to physical characteristics of materials, the identification of pigments and its spatial distribution across the painting is now possible. In this work, The Scream (1893) by Edvard Munch is acquired using a hyperspectral scanner and the pigment mapping of its constituent pigments are carried out. Two spectral image classification methods, i.e. Spectral Angle Mapper (SAM) and Spectral Correlation Mapper (SCM), and a fully constrained spectral unmixing algorithm combined with linear mixing model are employed for the pigment mapping of the painting.

1 Introduction

In painting conservation field, obtaining physical and chemical properties of the constituent materials of paintings is substantial as such information enables conservators to file a thorough and faithful documentation of the painting, conduct historical study, plan and undertake conservation treatment, etc. Traditionally, the identification and analysis of materials, e.g. pigments, binder, substrate, etc., are carried out by the so-called invasive methods, where micro-samples of materials need to be taken out of the painting to undergo various analysis [4–6]. Although the removal of these micro-samples are controlled in such a way that it will not alter the works of art, e.g. by taking samples from loosely adhering areas of the painting [6], such methods are invasive per se. Moreover, micro-sample analyses are limited to the number of samples. Due to this limitation, the preparation of samples for the analyses should be performed and recorded very carefully in order to have samples that are representative of the problem at hand and the result of the analyses will only be giving a very limited information as opposed to the abundant information available in the whole painting.

VASARI, an EU funded project started in 1989, introduced multispectral imaging as a new non-invasive method for the purpose of accurate color documentation as recording method for paintings [10]. This imaging technology, originally developed for remote sensing applications, has the ability to capture both

---

* Is currently a Ph.D student at Gjøvik University College and University of Poitiers.

A. Elmoataz et al. (Eds.): ICISP 2014, LNCS 8509, pp. 247–256, 2014.

spatial and spectral information of objects. Ever since the success of VASARI and its successor, CRISATEL [13], multispectral imaging technology has been explored extensively for conservation of art [1,3,12]. There is, however, a limitation to multispectral imaging, i.e. it only covers several numbers of broad and not contiguous spectral bands. And due to this, the selection of bands is crucial and mostly the result is not of sufficient spectral resolution.

The main limitation of multispectral imaging is overcome by hyperspectral imaging technology. Hyperspectral imaging is defined as simultaneous acquisition of spatially coregistered images, in many, spectrally contiguous bands, measured in calibrated radiance units. Hence, for every spatial location in the image captured by a hyperspectral scanner, a complete spectrum corresponding to material contents are also obtained. With this ability, we can now identify and analyse materials composing a painting in a more accurate and detailed way than multispectral imaging. Furthermore, as hyperspectral imaging technology has been fully developed and matured in remote sensing field, methods and measures can be borrowed and adapted to applications in painting conservation, e.g. pigment mapping of paintings can be solved in a similar fashion as mineral mapping in remote sensing field.

This paper presents the pigment mapping of one of the paintings by Edvard Munch, i.e. The Scream (1983) [16]. Hyperspectral acquisitions of the painting has already been performed and reported [7]. Classification and spectral unmixing approaches are used to solve the pigment mapping task, and will be the main focus of this paper.

2 Methodology

2.1 Acquisition

Hyperspectral image acquisition of the painting has been performed by using a pushbroom scanner HySpex from Norsk Elektro Optikk [7,11]. The painting is illuminated by quartz enveloped halogen-tungsten broad-band light source which covers the spectral region 400-2500 nm. The line scanner and light sources are mounted in an X-Y translation stage, whose movements can be accurately controlled in horizontal and vertical directions and also synchronized with camera parameters. The painting is kept on a mounting frame, parallel to the translation stage at a distance matching with the focal point of the scanner's optics. The field of view is 10 cm, at a working distance of 30 cm. The painting size (91×73.5) cm^2 which is more than the field of view of the camera, it is necessary to move the scanner in both directions in order to acquire spectral data from whole painting. The illumination was carefully adjusted, to minimise heat development on the painting surface and its total exposure to light. In order to reduce the noise in the dataset, every line is captured several times and the values averaged before moving to the following line. For normalisation and to calibrate the spectral distribution of the light source to yield spectral reflectance data, an additional calibration target is captured, which is fixed in the same mounting frame, but outside the actual painting. This calibration target is spatially uniform and with a known spectral reflectance (50% Spectralon®). Post-processing steps for the radiometrically calibration which takes multiple influences into account is done automatically by the camera software [11].

2.2 Data

Reflectance Cube. Due to the positioning of the hyperspectral scanner during the acquisition of the painting, 3 VNIR reflectance cubes are obtained, each showing a fragment of the complete painting. Each of these cubes are of 1600-by-6805 pixels and 160 spectral bands (414.6 to 992.5 nm, in 3.6 nm interval). However, considering the noise level at the first and last 10 bands, only 140 spectral bands are used for the pigment mapping.

Spectral Library. Spectral library is a collection of reflectance spectra of pigments that are used in the painting by the artist. Singer et al. [15] carried out a pigment identification on the painting using invasive techniques, providing the information of constituent pigments and its corresponding location. Considering these locations as reference points, a spectral library is built by averaging spectral reflectances of pigments in the approximate referred location. Another spectral library of pigments of the same type that was found on the painting is built using Kremer pigments [8]. The pigments were applied on acid-free paper by screen-printing in water-soluble binder made of gum Arabic, i.e. a medium which is mostly used in watercolor technique where pure pigments are more often used and it hardly changes the color of the pigments. The list of pigments from both the painting and Kremer color charts are given in Table 1.

Table 1. List of pigments which are used to build spectral libraries needed in this study

Source	Pigment composition
In-situ pigments, obtained from spectral images of the painting referring to locations mentioned in Singer et al. [15].	Vermilion, gypsum 'Blue crayon': Ultramarine blue, gypsum 'Green crayon': Viridian, clay, zinc yellow, Prussian blue Cadmium yellow Lead white, zinc white, ultramarine blue Signature of painting substrate, i.e. cardboard
Kremer pigments, obtained from spectral images of Kremer pigment charts [8].	Prussian blue, ultramarine blue, cadmium yellow, viridian green, iron oxide red, and vermilion. Water-soluble binder made of gum Arabic was used for the application of each pigment.

2.3 Methods

Spectral Angle Mapper (SAM). Given the spectral data in terms of its reflectance, SAM classification method treats spectra as vector with dimensionality equals to the number of bands. SAM measures the similarity between target and reference spectra, t_λ and r_λ respectively, by calculating the angle between them [9], see eq. 1. The values of α are expressed in radians and of range [0, π], with smaller values correspond to higher similarity between two spectra. The output to this algorithm is binary pigment maps that give the information of pigment distribution across the painting.

$$\alpha = \cos^{-1}\left(\frac{\sum_\lambda t_\lambda r_\lambda}{\left(\sum_\lambda t_\lambda^2\right)^{1/2}\left(\sum_\lambda r_\lambda^2\right)^{1/2}}\right) \tag{1}$$

Spectral Correlation Mapper (SCM). SCM is said to be the improvement of SAM [2]. It calculates similarity between spectra in terms of their correlation, by using Pearsonian correlation coefficient. While the function, see eq. 2, is similar to that of SAM, the main difference is that SCM centralizes the data in its mean. Values of R range between -1 and 1; the value 1 means total correlation between spectra. As a classification algorithm, SCM returns binary pigment distribution maps across the painting.

$$R = \frac{\sum_\lambda (t_\lambda - \overline{t})(r_\lambda - \overline{r})}{\left(\sum_\lambda (t_\lambda - \overline{t})^2\right)^{1/2}\left(\sum_\lambda (r_\lambda - \overline{r})^2\right)^{1/2}} \tag{2}$$

Fully Constrained Spectral Unmixing. In spectral unmixing, given a target spectrum and a spectral library of pigments, the algorithm will try to find different mixtures of pigments from the spectral library that will give the best estimate. Because of this, not only spatial distribution of pigments is obtained, but also their abundance or concentration in every spatial location in the painting, resulting in gray scale pigment maps as output. In addition, an error map of estimating mixtures will also be given.

Finding the concentration of constituent pigments in a painting can be defined as constrained or unconstrained problem. A fully constrained spectral unmixing [14] requires sum to unity property for the constituent concentrations c_i, $i = 1, 2, \cdots, m$ of every pixel and that each fraction lie between 0 and 1 (eq. 3). Fully constrained spectral unmixing is used to be able to obtain concentration of pigments in terms of their percentage in the mixture. Also, unmixing algorithm is be combined with linear mixing model.

$$\sum_{i=1}^{m} c_i = 1, 0 \leq c_i \leq 1, i = 1, 2, \cdots, m \tag{3}$$

Exhaustive search approach [17] is used for the implementation of fully constrained spectral unmixing using linear mixing model assumption. Concentration of each pigment in the mixture is defined as between 0-100% in 5% steps. And as this exhaustive search algorithm tends to mix a large number of pigments and therefore increases the computation time, we limit the maximum number of pigments in the mixture to 3.

2.4 Evaluation

A pigment chart from Kremer [8] is used to compare accuracy of SAM and SCM classification. The result of classifying the color charts into its known constituent pigments will be the justification of which classification algorithm is better.

As for the pigment mapping of the painting, since there is no ground truth data available for all spatial locations in the painting, the use of ground truth information found in Singer et al. [15] as validation is of limited use. Therefore, in addition to that, the result is also justified and validated by experts in the field, i.e. responsible conservators of the painting.

The evaluation of the result of pigment unmixing of the painting imposes yet a more challenging task. However, for this purpose, Singer et al. [15] provides a really valuable information which tells us not only information about a single pigment, but also its mixture. Furthermore, the unmixing algorithm provides an estimation error map, given in terms of root mean square error.

3 Results and Discussion

3.1 Comparison of SAM and SCM

To compare the performance and accuracy of both SAM and SCM, vermilion is used as a classification target given a pigment chart consisting of several different pigments, see fig. 1(a). The threshold α and R of SAM and SCM respectively are set to $\alpha = \arccos(R) = 0.1$ radians.

Looking at the results of both SAM and SCM, see fig. 1, it is clear that SCM is superior to SAM which erroneously detects other pigments as vermilion. For real spectral reflectance data SAM can only detect and therefore present variations between 0° and 90° of angle. Or in other words, it is unable to detect negative correlation between spectra, which then leads to false detection as shown in our result. Giving a lower threshold $\alpha = 0.05$ radians for SAM does reduce the amount of false detections but at the same time also reduce the recognition of vermilion, which conclude its limited ability to give correct classification. On the other hand, by using Pearsonian correlation coefficient, SCM is able to differentiate between negative and positive correlation between spectra, thus resulting in better classification result.

3.2 Pigment Classification

Knowing that the in-situ pigments, see Table 1, are of much more complex composition due to the different painting technique which are not fully understood

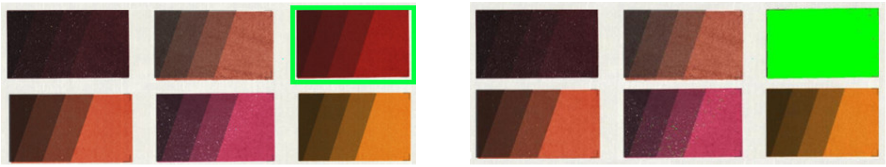

(a) Vermilion as target

(b) SCM result, $\arccos(R) = 0.1$

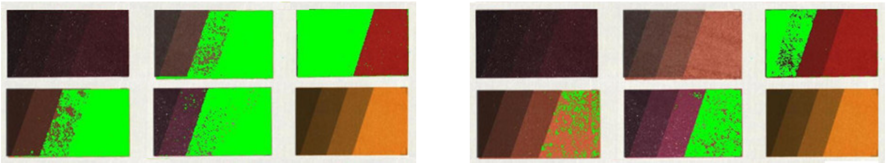

(c) SAM result, $\alpha = 0.1$

(d) SAM result, $\alpha = 0.05$

Fig. 1. SAM and SCM are used to identify vermilion on a red pigment chart, i.e. the pigment shown inside the green square. Regions with vermilion detection is colored green.

yet and for the fact that it has aged and deteriorated, spectral library consisting only of in-situ pigments are used in this SCM approach. Using the same parameter as the previous experiment of comparing SAM and SCM, some results are obtained and the results for vermilion and cadmium yellow are shown in fig. 2, target and result images are shown side by side. Looking at the result, it can be observed that SCM with $\arccos(R) = 0.1$ radians generally works well with vermilion and cadmium yellow, as regions pointed by the red arrows are correctly classified. However, by observing results obtained for other pigments, it is found that this particular threshold does not give good results for all pigments, e.g. blue and green crayon. To see whether giving different threshold would give better result at recognizing blue and green crayon, a higher threshold $\arccos(R) = 0.64$ radians is used and the result is as shown in fig. 3. The presence of the two pigments are relatively easy to evaluate visually in this figure, i.e. regions with the light blue and green strokes for blue and green crayon respectively. The results show that this particular threshold is suitable for green crayon but leads to some erroneous detections for blue crayon.

All the previous results for different pigments using different thresholds suggest that correlation level between pigments are different. For vermilion and cadmium yellow, the threshold of $\arccos(R) = 0.1$ radians was able to separate these pigments from other pigments or mixtures. But it was certainly not the case for blue and green crayon, which needed higher threshold. Therefore as what these results have suggested, for the future improvements, different class of pigments will have different threshold which then leads to using a multiple threshold SCM algorithm.

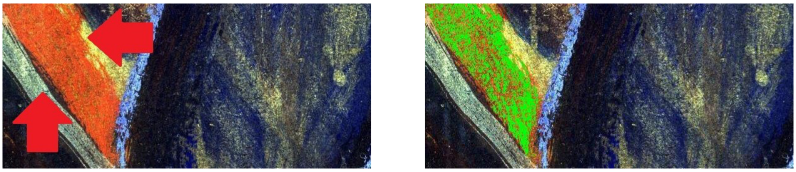

(a) Target: vermilion (b) Result: vermilion

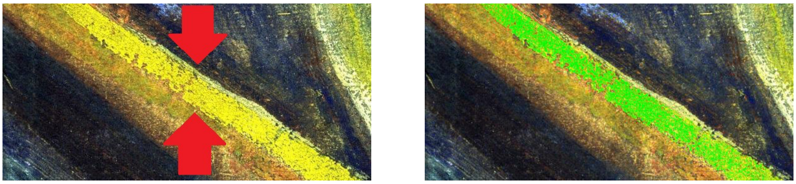

(c) Target: cadmium yellow (d) Result: cadmium yellow

Fig. 2. A fragment of the painting is shown for vermilion and cadmium yellow as classification target, whose locations are pointed by the red arrows. The classification result is also given where detected regions are overlaid with green color.

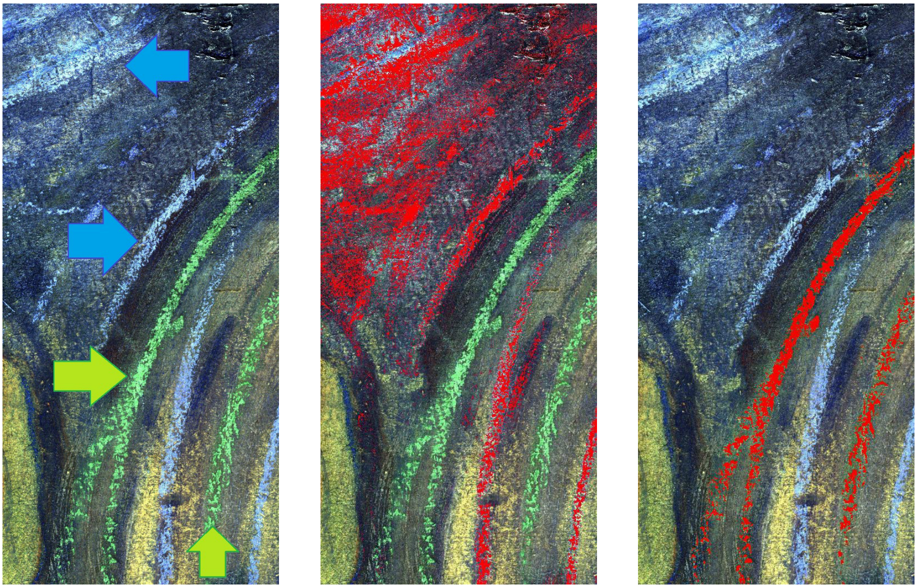

(a) Target: blue and green crayon (b) Result: blue crayon (c) Result: green crayon

Fig. 3. A fragment of the painting is shown for blue and green crayon as classification target, pointed by the blue and green arrows respectively. The classification result is also given where detected regions are overlaid with red color.

3.3 Pigment Spectral Unmixing

Fig. 4 shows a result for the case of vermilion obtained from the fully constrained spectral unmixing algorithm using 12 pigments listed on Table 1. Knowing that the orange/ red colored regions pointed by the red arrows in fig. 4(a) are locations with vermilion occurrences, detections of vermilion in these regions are to be expected. Eventhough SCM classification method does recognize vermilion in these regions in fig. 4(b), the unmixing algorithm provides much more information in fig. 4(c). Unmixing result says that other than those regions, vermilion is also found in other places together with other pigments composing a mixture. In fact, these regions where vermilion was found to be part of a mixture, being less than 100% of concentration, are regions where SCM failed to recognize it as any of the pigments because these regions are of highly mixed pigments. The limitation of SCM, i.e. its ability to work well only on homogeneous region, is therefore overcome by the unmixing approach since it is able to indicate not only the presence but also the abundance of pigments. In total, the unmixing approach was able to detect that vermilion is present on the painting at several concentrations, i.e. 0%, 5%, 10%, 90%, 95%, and 100%. As mentioned previously, due to the absence of ground truth data, the evaluation of these results is done through the estimation error given by the algorithm. Using root mean square error metric, the highest and lowest error values are 13.12% and 0.7% with average value of 2.65%.

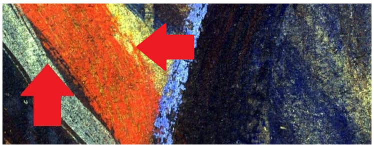

(a) Target image

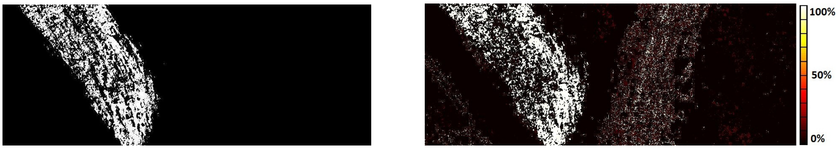

(b) SCM map (c) Abundance map

Fig. 4. A fragment of the painting and an abundance map for an in-situ vermilion, see Table 1. In the abundance map, the closer the color to white, the more percentage it has in the pigment mixture

4 Conclusion and Future Works

A pigment chart was initially used to compare the accuracy of SAM and SCM. SCM was found to be superior to SAM, as it enabled detection of negative correlation between spectra, and thus was used as the classification method for pigment mapping of the painting. SCM with threshold of $\arccos(R) = 0.1$ radians worked generally well for vermilion and cadmium yellow, but not for all especially the crayon pigments. This problem calls for setting a different threshold for different type of pigments, as different types of pigments have different correlation level.

Since SCM classification method is only suitable for homogeneous region, it failed at classifying highly mixed regions, hence the spectral unmixing approach. Fully constrained spectral unmixing algorithm combined with a linear mixing model was employed to estimate pigment mixture. This approach showed some interesting results, where regions unrecognized by SCM were recognized as mixture of some percentage of different pigments. In this algorithm, even though correctness of the estimate was not quantifiable, estimation accuracy was provided for every spatial location in the image. The average estimation accuracy given the case of using 12 in-situ and Kremer pigments (see Table 1) was 2.65%. However, linearity assumption in the mixing model that was used was not actually satisfied since the spatial resolution of the acquisition of the painting was really high. Moreover, not only optical mixing but also chemical mixing happened in the scene that was captured. Therefore, for future work, pigment mixing models that can describe both optical and chemical interaction between materials in the scene are needed to be able to accurately estimate the best mixture of pigments for the painting.

References

1. Baronti, S., Casini, A., Lotti, F., Porcinai, S.: Segmentation of multispectral images of works of art through principal component analysis. In: Del Bimbo, A. (ed.) ICIAP 1997. LNCS, vol. 1310, pp. 14–21. Springer, Heidelberg (1997)
2. de Carvalho Jr., O.A., Meneses, P.R.: Spectral correlation mapper (SCM): An improvement on the spectral angle mapper (SAM). Summaries of the 9th JPL Airborne Earth Science Workshop 1, pp. 65–74 (2000)
3. Casini, A., Lotti, F., Picollo, M.: Imaging spectroscopy for the non-invasive investigation of paintings. In: International Trends in Optics and Photonics, vol. 74, pp. 343–356. Springer, Heidelberg (1999)
4. Chalmin, E., Vignaud, C., Menu, M.: Palaeolithic painting matter: natural or heat-treated pigment? Applied Physics A 79(2), 187–191 (2004)
5. Chiavari, G., Fabbri, D., Prati, S., Zoppi, A.: Identification of indigo dyes in painting layers by pyrolysis methylation and silylation. A case study: "The Dinner of Emmaus" by G. Preti. Chromatographia 61(7-8), 403–408 (2005)
6. Edwards, H.G.M., Farwell, D.W., Brooke, C.J.: Raman spectroscopic study of a post-medieval wall painting in need of conservation. Analytical and Bioanalytical Chemistry 383(2), 312–321 (2005)
7. Hardeberg, J.Y., George, S., Deger, F., Baarstad, I., Palacios, J.E.H.: Spectral Scream: Hyperspectral image acquisition and analysis of a masterpiece. In: Frøysaker, T., Streeton, N., Kutzke, H., Topalova-Casadiego, B., Hanssen-Bauer, F. (eds.) Public Paintings by Edvard Munch and some of his Contemporaries. Changes and Conservation Challenges. Archetype Publications (2014)
8. Kremer Pigmente GmbH & Co. KG: 990001 – 990018 color charts (2013), `http://www.kremer-pigmente.com/en/`

9. Kruse, F., Lefkoff, A., Boardman, J., Heidebrecht, K., Shapiro, A., Barloon, P., Goetz, A.: The spectral image processing system (SIPS)- interactive visualization and analysis of imaging spectrometer data. Remote Sens. Environ. 44(2-3), 145–163 (1993)
10. Martinez, K.: High resolution digital imaging of paintings: The Vasari Project. Microcomputers for Information Management 8(4), 277–283 (1991)
11. Norsk Elektro Optikk AS: HySpex, `http://www.neo.no/hyspex/`
12. Novati, G., Pellegri, P., Schettini, R.: An affordable multispectral imaging system for the digital museum. Int. Journal on Digital Libraries 5(3), 167–178 (2005)
13. Ribés, A., Schmitt, F., Pillay, R., Lahanier, C.: Calibration and spectral reconstruction for CRISATEL: An art painting multispectral acquisition system. Journal of Imaging Science and Technology 49(6), 563–573 (2005)
14. Robinson, G.D., Gross, H.N., Schott, J.R.: Evaluation of two applications of spectral mixing models to image fusion. Remote Sens. Environ. 71, 272–281 (2000)
15. Singer, B., Aslaksby, T., Topalova-Casadiego, B., Tveit, E.S.: Investigation of materials used by Edvard Munch. Studies in Conservation 55, 1–19 (2010)
16. Woll., G.: Edvard Munch: Complete paintings, London, vol. 1-4, p. 333 (2009)
17. Zhao, Y.: Image segmentation and pigment mapping of cultural heritage based on spectral imaging. Ph.D. thesis, Rochester Institute of Technology (2008)